JOURNAL OF MATERIALS SCIENCE 26 (1991) 3769 - 3774

Microstructure and mechanical properties of hot-pressed SiC–TiC composites

H. ENDO, M. UEKI, H. KUBO
R and D Laboratories-I, Nippon Steel Corporation, 1618 Ida, Nakahara-ku, Kawasaki 211, Japan

Hot-pressed SiC–TiC composite ceramics with 0–100 wt % TiC have been investigated to determine the effect of composition (amount of TiC) on the elastic modulus, hardness, flexural strength and fracture toughness, K_{IC}. The composites exhibited superior mechanical properties compared to monolithic SiC and TiC, especially in fracture toughness, K_{IC}, value for 30–50 wt % TiC composite. The maximum values of K_{IC} and room-temperature flexural strength were 6 MPa $m^{1/2}$ for a 50 wt % TiC and 750 MPa for a 30 wt % TiC composite, respectively. The observed toughening could be attributed to the deflection of cracks due to dispersion of the different particles. Although no third phases were detected by both TEM and XRD studies, an EDAX study and resistivity measurements indicated some possibility of solid solutions being present. The composites containing more than 30 wt % TiC, exhibited resistivity lower than 10^{-3} Ω cm which is favourable for electro-discharge machining of ceramics.

1. Introduction

SiC-based ceramics have been known as materials with high strength and excellent wear resistance at high temperatures; however, they exhibit poor reliability due to low fracture toughness, K_{IC}. Recently, incorporation of some other non-oxide materials into the SiC-based ceramics has been widely investigated to solve the above problems. Among these non-oxide materials, compounds (carbides, nitrides and borides) of elements belonging to the IVa, Va and VIa groups of the Periodic Table which are exemplified by TiC and TiB_2, have been paid attention from the aspect of high refractoriness and hardness with lower resistivity compared to the metallic materials.

Investigations concerned with toughening and lowering the resistivity of SiC by incorporating these compounds, are increasing in number. Wei and Becher [1] have reported that incorporation of TiC into SiC in the range up to 24.6 vol % increased the toughness of monolithic SiC to a maximum of 6 MPa $m^{1/2}$ (1.5 times). The four-point flexural strength of the composites had a maximum value of 680 MPa, and they used 1 wt % Al and 1 wt % C as sintering aids for SiC in hot pressing. Janney [2] used phenolic resin as a C source for sintering SiC–TiC composites. The procedure offered homogenization of the microstructure, resulting in a significant increase in reliability (Weibull modulus). Janney [3] and McMurtry *et al.* [4] have studied SiC–TiB_2 system composites with the addition of B and C as sintering aids. In the former, the SiC–15 vol % TiB_2 (0.5% B–1% C) composite was fabricated by hot-pressing at 2000 °C. The hot-pressed material recorded a fracture toughness of 4.5 MPa $m^{1/2}$ (Indentation microfracture (IM) method, 1.45 times higher than monolithic SiC) and a flexural strength of 485 MPa. In the latter case pressureless sintering at temperatures higher than 2000 °C was tried for SiC–16 vol % TiB_2 composite. Fracture toughness of the sintered body was as high as 8.9 MPa $m^{1/2}$ (single edge-notched beam (SENB) method) with a four-point flexural strength of 480 MPa and a resistivity lower than 1 Ω cm.

Matsushita *et al.* [5–7] have reported that composites of SiC with 50 vol % TiC, WC, ZrB_2, TiB_2, HfB_2, NbB_2, TaB_2 and TiN, and SiC–0 to 80 vol % ZrB_2 (with the addition of 2 wt % Al_2O_3) exhibited resistivity in the range 0.13–10^{-5} Ωcm, and the resistivity of such composites could be controlled by changing the amount of the electro-conductive material described above. These ceramics are expected to be applied as heating elements and igniters.

In the present study, as continuation of previous works [8, 9], the mechanical properties (flexural strength, fracture toughness, elastic modulus and hardness), resistivity and microstructure were investigated for hot-pressed SiC–TiC ceramics with the incorporation of 0–100 wt % TiC, together with B_4C and C as sintering aids.

2. Experimental procedure

The starting powders used to fabricate the SiC–TiC composites are listed in Table I with their particle size, purity and manufacturer. Powders of β-SiC and TiC were mixed with B_4C powder and carbon black as sintering aids for SiC. The range of TiC addition to the SiC was from 0 (monolithic SiC) to 100 wt % (monolithic TiC). Well-mixed powders were attained by ball-milling in *n*-hexane for 24 h using polyamide media. After drying, the powders were loaded into a graphite

0022–2461/91 $03.00 + .12

TABLE I Particle size, purity and manufacturer of the starting powders

Starting powder	Average particle size (μm)	Purity (%)	Manufacturer and grade
β-SiC	0.3	> 98	Ibiden Co. Ltd (Ultrafine)
TiC	0.4	> 99	Kojundo Chem. Lab. Co. Ltd
B_4C	1.2	> 99	Denki Kagaku Kogyo KK (1500A)
C (Carbon black)	0.02	> 99	Mitsubishi Chem. Ind. (600MA)

die with i.d. = 90 mm and hot-pressed at 2150 °C for 2 h under a pressure of 40 MPa in an Ar gas atmosphere. Hot-pressed discs of SiC–TiC composites were machined into pieces (3 mm × 4 mm × 38 mm) for flexural tests and the densities were measured by a water displacement method. Three-point flexural tests were conducted at room and elevated temperatures (at 1500 °C under the dynamic flow of Ar gas), according to the method specified as JIS R-1601 and R-1604, respectively. The fracture toughness, K_{IC}, was determined by using a single-edge pre-cracked beam (SEPB) method [10]. Elastic moduli of SiC–TiC composites were also examined using a pulse-echo-overlap method. The resistivity of the composites was measured by using apparatus equipped with four probes. In the apparatus the disturbance due to the contact resistance between the specimen and the probe could be subtracted from the results of the experiment. Microstructural features of the composites were examined by X-ray and electron diffractometries in conjunction with optical, scanning and transmission electron microscopy.

3. Results and discussion

3.1. Microstructural observation

A transmission electron micrograph of hot-pressed (at 2150 °C) SiC–50 wt % TiC (–0.5 wt % B–1 wt % C) is shown in Fig. 1, indicating a uniform microstructure with equiaxed grains that range in size between 2 and 5 μm. In the micrograph the formation of third phases such as TiB_2 which could be formed by the reaction between TiC and B_4C, were not observed. The mapping pictures obtained from the energy dispersive analysis of X-rays (EDAX) are also attached to the micrograph. Neither of the features of Si from SiC and Ti from TiC overlapped each other. This means that particles of SiC and TiC exist separately and are dispersed relative to each other. Although no phases other than β-SiC and TiC were detected by X-ray diffractometry, the results of more detailed EDAX study suggested some possibility that formation of a solid solution between SiC and TiC had occurred. Fig. 2 shows the EDAX spectrums obtained from SiC and TiC grains in the composite. Even though they were very weak, the peaks representing Ti and Si were detected from the spectra for SiC and TiC, respectively. It may indicate that there is a possibility that a solid solution of SiC with TiC exists in the composite. Nevertheless, those peaks may have appeared due to influence from the surrounding grains . The β-SiC has the crystalline form of 3C (zinc blende type) with a lattice parameter of $a = 0.436$ nm and TiC has that of simple cubic (NaCl type) with $a = 0.433$ nm. The crystalline form and the lattice parameter of both grains are similar to each other, indicating rather easy formation of solid solution between them.

3.2. Compositional dependence of elastic modulus and hardness

Fig. 3 shows the elastic modulus, E, and Poisson's ratio, ν, of the SiC–TiC composite as a function of TiC

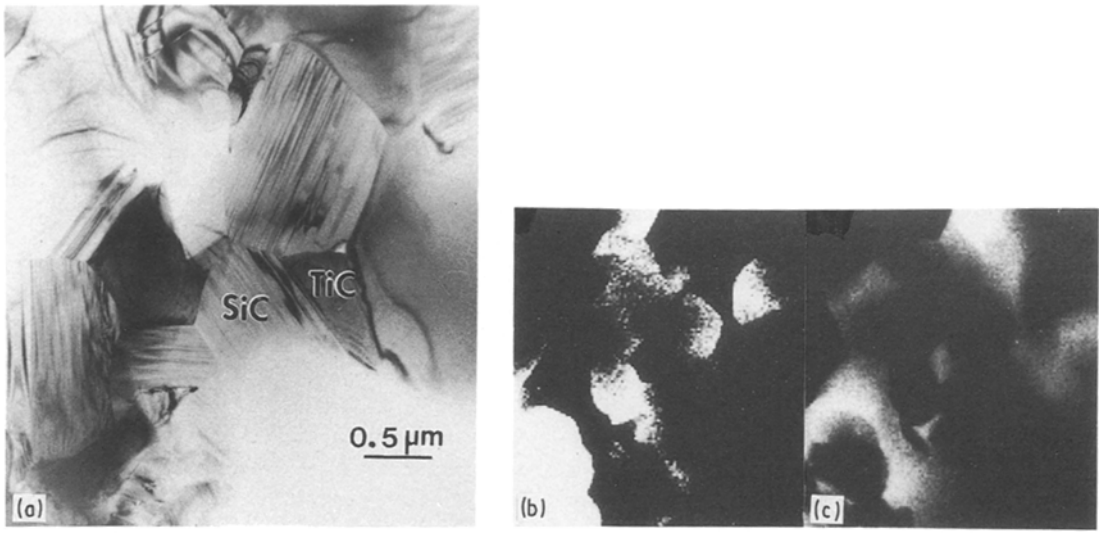

Figure 1 (a) Transmission electron micrograph, and mapping pictures for (b) Si and (c) Ti, obtained from EDAX of SiC–50 wt % TiC composite hot-pressed at 2150 °C.

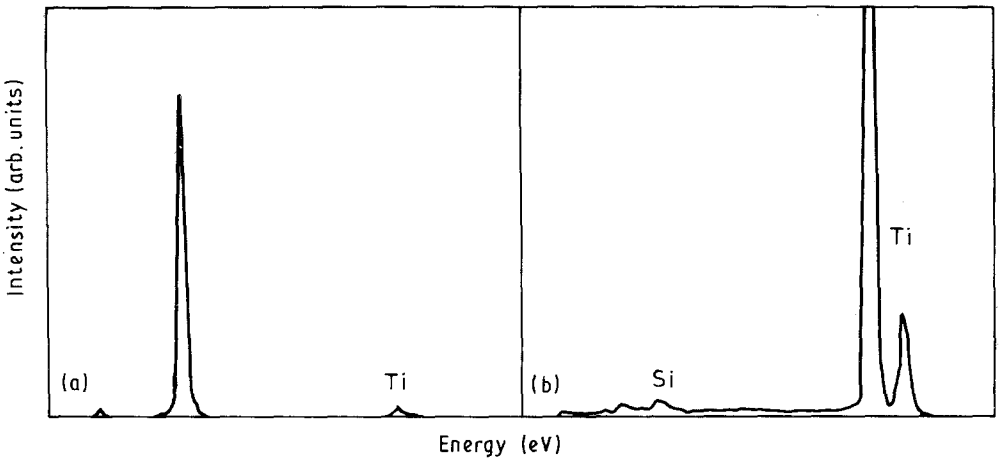

Figure 2 EDAX spectrums obtained from (a) SiC and (b) TiC grain in the SiC–50 wt % TiC composite hot-pressed at 2150 °C.

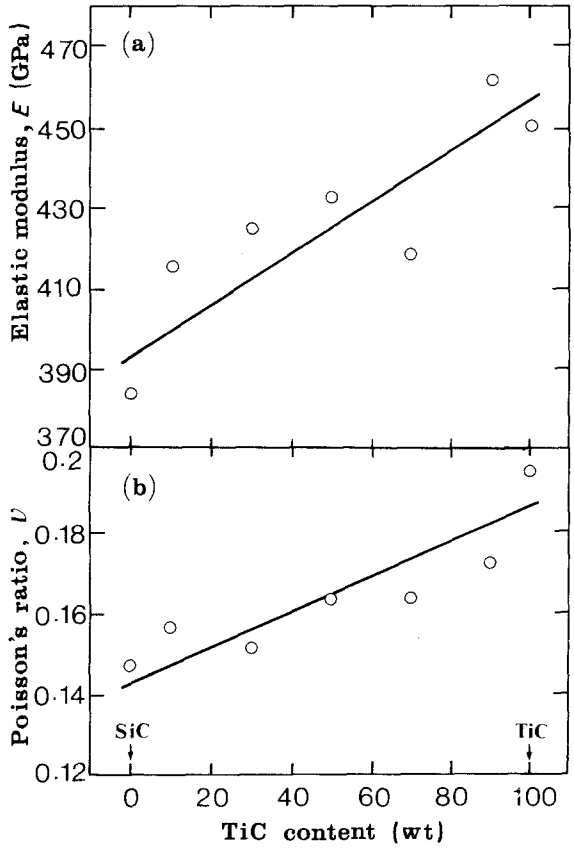

Figure 3 Dependence of (a) elastic modulus, E, and (b) Poisson's ratio, v, of the SiC–TiC composites on the content of TiC. Hot pressed at 2150 °C, 2 h, 40 MPa.

content. Both E and v for the composites increased linearly with addition of TiC from 3.9 GPa (3.9 $\times 10^{11}$ N m^{-1}) and 0.145 for SiC, to 4.5 GPa (4.5 $\times 10^{11}$ N m^{-1}) and 0.195 for TiC. The values of both monolithic ceramics agreed well with the values listed in the data book [11, 12], and the moduli for the composites fitted well on a line connecting the values for both the monolithic ceramics, suggesting that the so-called composite law was almost observed. These experimental results verify the fact that any third phase, such as a reaction product or a grain-boundary phase, has not formed.

During the hardness measurements, because monolithic TiC and the TiC-rich composites exhibited a delayed fracture for loads higher than 1 kgf, (1 kgf = 9.8067 N), a micro-Vickers tester was used for the measurements with a load of 0.5 kgf. Fig. 4 shows the variation of the hardness with the TiC content. For all the compositions, the composites exhibited quite high hardness with $H_v = 2500$ or more. As one of the reasons for exhibiting a slightly lower hardness value ($H_v = 2650$) than that presented (H_v 3000) for the sintered TiC in the data book [11, 12], the occurrence of grain coarsening during sintering was considered. The reason for the slightly lower hardness values exhibited by the composites compared to the monolithic SiC was considered to be caused by the residual stress field generated in the sintered composite material due to the thermal expansion coefficient mismatch.

3.3. Flexural strength

Fig. 5 shows the composition dependence of the three-point flexural strength of the SiC–TiC composites at room and elevated temperatures (1500 °C in Ar gas

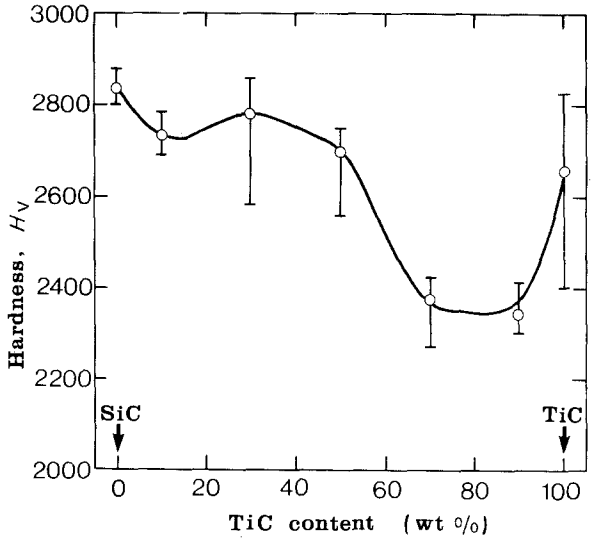

Figure 4 Variation of the hardness of SiC–TiC composites with TiC content. Hot pressed at 2150 °C, 2 h, load 0.5 kgf.

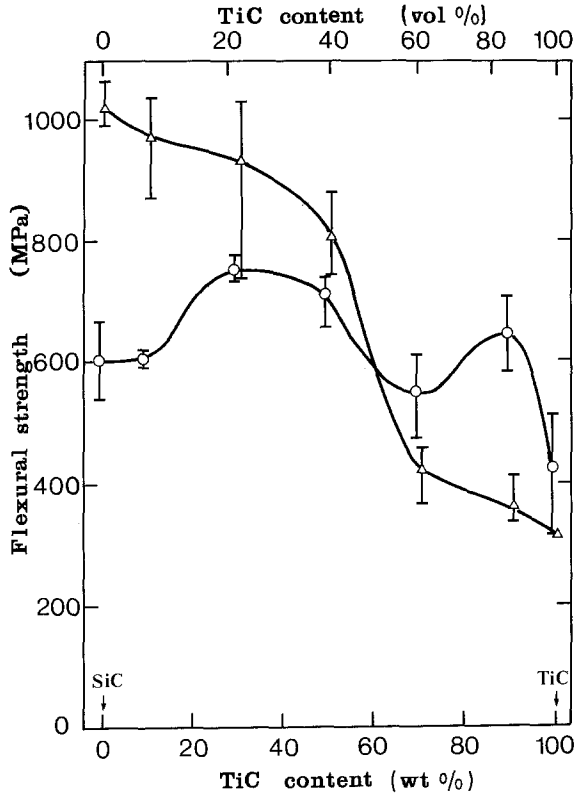

Figure 5 Composition dependence of the three-point flexural strength of the SiC–TiC composites hot-pressed at 2150 °C at (○) room (△) elevated (1500 °C in Ar) temperatures.

atmosphere). The flexural strengths for both hot-pressed (at 2150 °C) monolithic SiC and TiC were 620 and 420 MPa, respectively. For the composites, strengths higher than 750 MPa were recorded for 30–50 wt % TiC composites. These results agreed well with the results on the composition dependence of the fracture toughness which is shown in Fig. 6. From these observations, it can be concluded that strengthening was achieved through toughening at least at room temperature. Furthermore, in addition to that, the incorporation of TiC into SiC and vice versa was

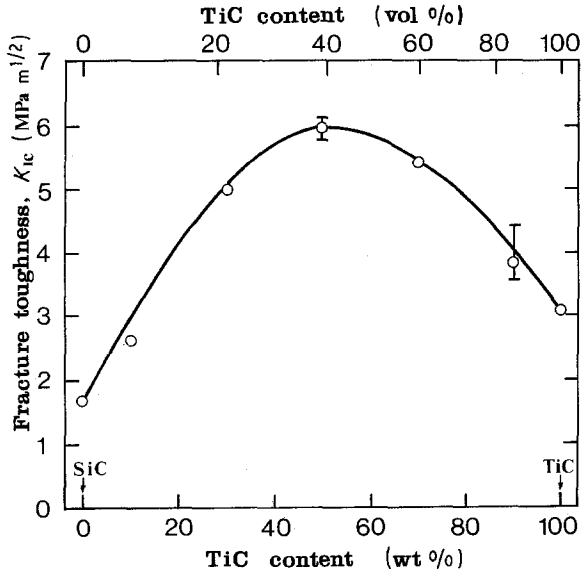

Figure 6 Variation of fracture toughness, K_{IC}, with the content of TiC in the SiC–TiC composites hot-pressed at 2150 °C.

effective for inhibiting grain growth of both phases. However, the strength at 1500 °C decreased monotonically with increasing TiC content from 1000 (for monolithic SiC) to 300 MPa (for monolithic TiC). This is due to the lower strength of TiC than SiC at that temperature, and partly due to the plasticity of TiC at high temperatures. In fact, the composites containing large amounts of TiC did not exhibit brittle fracture behaviour in the load–deflection curve for the flexural tests at 1500 °C.

3.4. Fracture behaviour

Fig. 6 shows the variation of fracture toughness, K_{IC} with TiC content, exhibiting a maximum value of 6 MPa m$^{1/2}$ for a 50 wt % TiC composite in terms of the SEPB method. When the K_{IC} was measured by the IM method [13] the value was as high as 8.5 MPa m$^{1/2}$. The increase in K_{IC} by incorporating TiC into SiC and vice versa, can be attributed to the deflection of cracks due to dispersion of the different particles [14]. In Fig. 7 the crack propagation from the Vickers indentation was compared for hot-pressed monolithic β-SiC (–1 wt % B–1 wt % C) and β-SiC–50 wt % TiC composites. By incorporating TiC into SiC, the cracks were deflected considerably and consequently their propagation was inhibited in the case of the composite, while deflection rarely occurred in the monolithic SiC. The crack deflection was thought to be caused by the residual stress generated by the difference in the thermal expansion coefficient and elastic modulus between SiC and TiC in the composites [15]. Wei and Becher [1] have estimated the residual stress between SiC matrix and added TiC spherical particles in their composite, as the radial matrix stress of + 1000 MPa (tensile) and tangential matrix stress of − 500 MPa (compressive). The improvement in fracture toughness is, however, much higher than that expected from analytical [16] and computed [17] models. Therefore, other toughening mechanisms such as pinning, branching and bowing of cracks must be operating in the present composites.

3.5. Resistivity

In Fig. 8 resistivity for the composites is compared as a function of TiC content to those calculated by the following theoretical model [18]. Suppose the electrical conductivities for two kinds of fine particles are expressed by σ_1 and σ_2, respectively, the conductivity, σ, for a well-mixed composite of the two particles can be expressed as

$$\sigma = (3V_1 - 1)\sigma_1 + (3V_2 - 1)\sigma_2 + \{[(3V_1 - 1)\sigma_1 + (3V_2 - 1)\sigma_2]^2 + 8\sigma_1\sigma_2\}^{1/2})/4 \quad (1)$$

where V_1 and V_2 are the volume fractions of each particle. From the experimental results, only 10 wt % addition of TiC drops the resistivity of SiC dramatically. Thus, the resistivity can be optionally controlled in the range from 10^{-4} to 10^2 Ω cm by changing the content of TiC. The discrepancy observed between

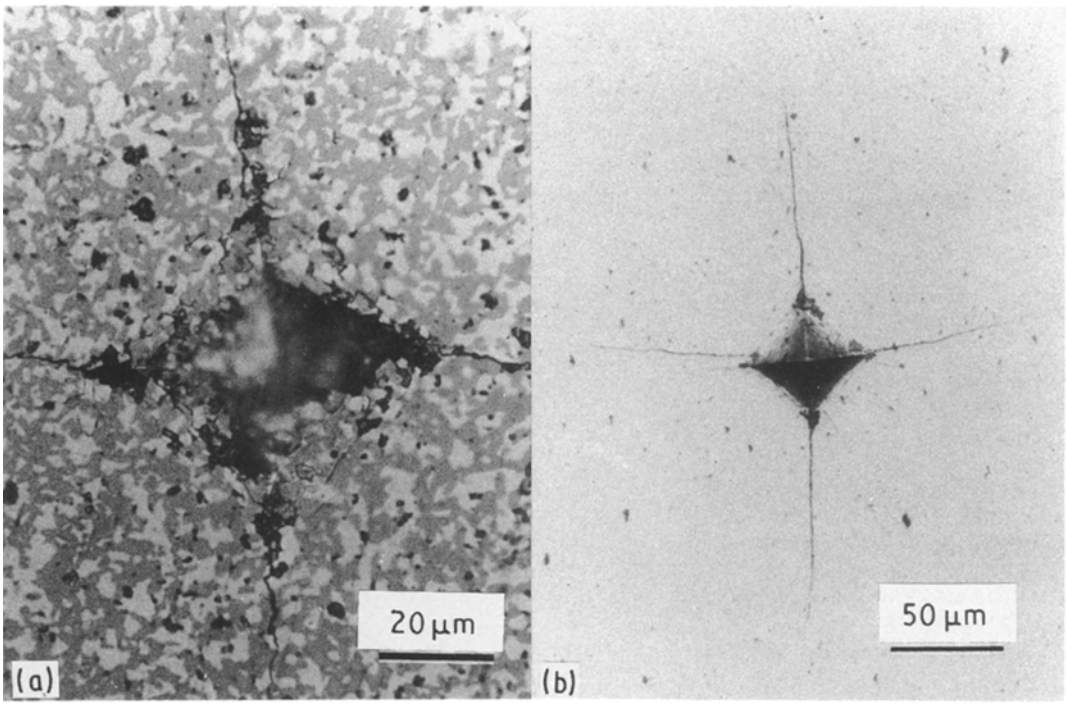

Figure 7 Comparison of the crack propagation from Vickers indentation for (a) SiC–50 wt % TiC composite and (b) β-SiC (–1 wt % B–1 wt % C) hot-pressed at 2150 °C.

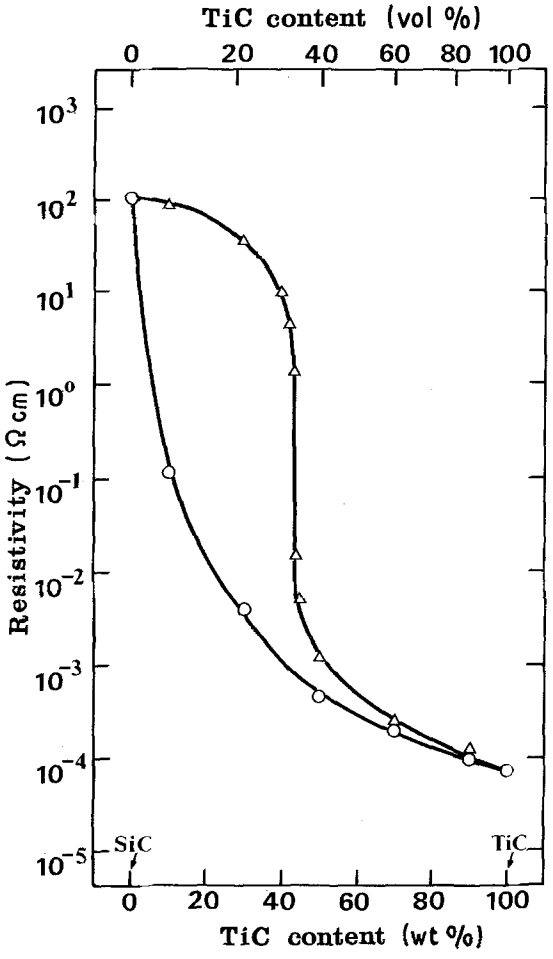

Figure 8 Comparison of (○) measured resistivity for the SiC–TiC composites with (△) the calculated values as a function of the TiC content.

the calculated and experimental results, especially at lower TiC contents, seems to be caused by inhomogeneity of the microstructure in the composites. However, the solid solutioning effect mentioned before may also cause such a discrepancy. The formation of TiC layers on the surface of SiC particles should have some influence on the electrical conductivity around the grain boundaries in the composite. The electrically conductive composites containing more than 30 wt % TiC exhibited superior machinability during electrodischarge machining.

4. Conclusions

In the hot-pressed SiC–TiC composites, although other phases were not detected by TEM or XRD studies, more detailed EDAX study suggested some possibility of the formation of a solid solution between SiC and TiC. Elastic modulus and Poisson's ratio for the SiC–TiC composites increased linearly with amount of TiC from 3.9 GPa and 0.145 for SiC to 4.5 GPa and 0.195 for TiC, respectively. The so-called composite law was closely followed, and these results denied the implication described above (i.e. possibility of the formation of a third phase).

The composites containing 30–50 wt % TiC exhibited flexural strengths exceeding 750 MPa at room temperature which, were higher than those of either SiC (620 MPa) or TiC (420 MPa). A more significant effect of TiC incorporation was observed in the fracture toughness measurements, namely, the SiC–50 wt % TiC exhibited the maximum value of 6 MPa $m^{1/2}$. The main reason for the toughening

could be attributed to the deflection of cracks due to dispersion of the different particles.

In the composites, the resistivity could be controlled in the range from 10^{-4} to $10^{2}\ \Omega$cm by changing the proportion of TiC in the composite. From the discrepancy observed between the calculated and experimental results at especially low TiC content, the possibility of solid solutioning was indicated.

References

1. G. C. WEI and P. F. BECHER, *J. Amer. Ceram. Soc.* **67** (1984) 571.
2. M. A. JANNEY, *Amer. Ceram. Soc. Bull.* **65** (1986) 357.
3. *Idem, ibid.* **66** (1987) 322.
4. C. H. McMURTRY, W. D. G. BOECKER, S. G. SESHADRI, J. S. ZANGHI and J. E. GARNIER, *ibid.* **66** (1987) 325.
5. Y. MATSUSHITA, K. NAKAMURA and K. HARADA, US Pat. 4 555 358 (1985).
6. R. JIMBOU, K. TAKAHASHI, Y. MATSUSHITA and T. KOSUGI, *Adv. Ceram. Mater.* **1** (1986) 341.
7. K. TAKAHASHI, R. JIMBOU, Y. MATSUSHITA, S. YAMADA and T. KOSUGI, *J. Jpn Ceram. Soc.* **93** (1985) 123.
8. H. ENDO, K. TANEMOTO and H. KUBO, "Sintering' 87". Vol. 2, edited by S. Somiya, M. Shimada, M. Yoshimura and R. Watanabe, (Elsevier, London, 1988) pp. 1052–7.
9. H. ENDO, M. UEKI and H. KUBO, *J. Mater Sci.*, **25** (1990) 2503.
10. T. NOSE and T. FUJII, *J. Amer. Ceram. Soc.* **71** (1988) 328.
11. G. V. SAMSONOV and I. M. VINIOKIO, "Tugoplavkie Soedineniya" (Metappurgiya, Moskva, 1976) pp. 58, 303.
12. "Engineering Property Data on Selected Ceramics", Vol. 2 "Carbides" (Metals and Ceramics Information Center, Battelle, Ohio, 1987) pp. 5.2.3–1 to 5.2.4.–26.
13. B. R. LAWN, A. G. EVANS and D. B. MARSHALL, *J. Amer. Ceram. Soc.* **63** (1980) 371.
14. A. G. EVANS, *Phil. Mag.* **26** (1972) 1327.
15. A. G. EVANS and T. G. LANGDON, *Prog. Mater. Sci.* **21** (1976) 171.
16. K. T. FABER, A. G. EVANS and M. D. DRORY, "Fracture Mechanics of Ceramics" Vol. 6, edited by R. C. Bradt, A. G. Evans, D. P. H. Hasselman and F. F. Lange (Plenum Press, New York, London, 1983) pp. 77–92.
17. S. G. SESHADRI, M. SHRINIVASAN and K. M. KEELER, *Ceram. Engng Sci. Proc.* **8** (1987) 671.
18. R. LANDAUER, *J. Appl. Phys.* **23** (1952) 779.

Received 16 January
and accepted 19 November 1990